THE JOURNAL OF PHYSICAL CHEMISTRY A

Article

pubs.acs.org/JPCA

Stabilizing *g*-States in Centrosymmetric Tetrapyrroles: Two-Photon-Absorbing Porphyrins with Bright Phosphorescence

Tatiana V. Esipova,[†] Héctor J. Rivera-Jacquez,[§] Bruno Weber,[∥] Artëm E. Masunov,[§,⊥,#,¶] and Sergei A. Vinogradov*[,†,‡]

[†]Department of Biochemistry and Biophysics, Perelman School of Medicine and [‡]Department of Chemistry, School of Arts and Sciences, University of Pennsylvania, Philadelphia, Pennsylvania 19104, United States

[§]NanoScience Technology Center, Department of Chemistry and Department of Physics, University of Central Florida, Orlando, Florida United States

[∥]Institute of Pharmacology and Toxicology, University of Zurich, Zurich CH-8057, Switzerland

[⊥]Photochemistry Center RAS, ul. Novatorov 7a, Moscow 119421, Russia

[#]South Ural State University, Lenin pr. 76, Chelyabinsk 454080, Russia

[¶]National Nuclear Research University MEPhI, Kashirskoye sh. 31, Moscow 115409, Russia

Supporting Information

ABSTRACT: Using time-dependent density functional theory (TDDFT) and sum-overstates (SOS) formalism, we predicted significant stabilization of 2P-active *g*-states in a compact fully symmetric porphyrin, in which all four pyrrolic fragments are fused with phathalimide residues via the *β*-carbon positions. The synthesis of a soluble, nonaggregating *meso*-unsubstituted tetraarylphthalimidoporphyrin (TAPIP) was then developed, and the spectroscopic measurements confirmed that a strongly 2P-active state in this porphyrin is stabilized below the B (Soret) state level. Single-crystal X-ray analysis revealed near-ideally planar geometry of the TAPIP macrocycle, while its tetra-*meso*-arylated analogue (*meso*-Ar_4TAPIP) was found to be highly saddled. Consistent with these structural features, Pt *meso*-Ar_4TAPIP phosphoresces rather weakly (ϕ_{phos} = 0.05 in DMF at 22 °C), while both Pt and Pd complexes of TAPIP are highly phosphorescent (ϕ_{phos} = 0.45 and 0.23, respectively). In addition PdTAPIP exhibits non-negligible thermally activated (E-type) delayed fluorescence ($\phi_{fl}(d) \sim 0.012$). Taken together, these photophysical properties make metal complexes of meso-unsubstituted tetaarylphthalimidoporphyrins the brightest 2P-absorbing phosphorescent chromophores known to date.

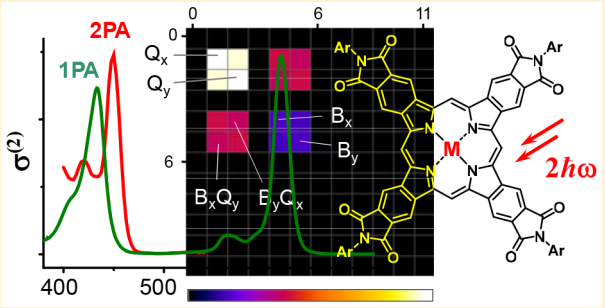

INTRODUCTION

In recent years interest in two-photon-absorbing tetrapyrroles capable of efficient generation of triplet states has been on the rise primarily due to their potential usefulness in targeted depth-resolved photodynamic therapy (PDT).[1−4] Extensive synthetic work aiming to enhance two-photon absorption (2PA) in porphyrin-based systems led to molecules with exceptionally high 2PA cross sections (see refs 5−7 for reviews and refs 8−19 for recent examples), simultaneously capable of singlet oxygen generation and in some cases retaining sufficiently strong fluorescence for imaging.[14,17,19] In contrast, triplet emissivity of the sensitizer molecules has never drawn much attention, since the basis for PDT is triplet-mediated photochemical action (oxygen sensitization), as opposed to emission of phosphorescence. Consequently, 2P-absorbing phosphorescent porphyrins remain poorly studied, while such molecules could be very useful as probes for two-photon phosphorescence lifetime microscopy (2PLM) of oxygen[20]—a recently developed imaging technique with applications already encompassing several branches of biology.[21−27]

The principal difficulty in achieving efficient 2P excitation of a porphyrin molecule originates in its centrosymmetric structure. The ground state wave functions of porphyrins are *gerade* (symmetric) with respect to the center of inversion. For centrosymmetric closed-shell systems one-photon (1P) electric dipole-allowed transitions originating in *gerade* states (*g*-states), such as the ground state, are allowed only into *ungerade* (antisymmetric) states (*u*-states), such as Q- and B- (or Soret) states in porphyrins (Figure 1).[28] These *u*-states, however, are forbidden for 2PA, which may occur only between states of equal parity: $g \rightarrow g$ or $u \rightarrow u$. Although in molecules symmetry selection rules are usually relaxed to some extent due to asymmetric vibrations, in rigid aromatic macrocycles, such as

Received: May 6, 2017
Revised: July 14, 2017
Published: August 2, 2017

Downloaded via UNIV OF ZURICH on February 10, 2024 at 17:42:51 (UTC).
See https://pubs.acs.org/sharingguidelines for options on how to legitimately share published articles.

© 2017 American Chemical Society

DOI: 10.1021/acs.jpca.7b04333
J. Phys. Chem. A 2017, 121, 6243−6255

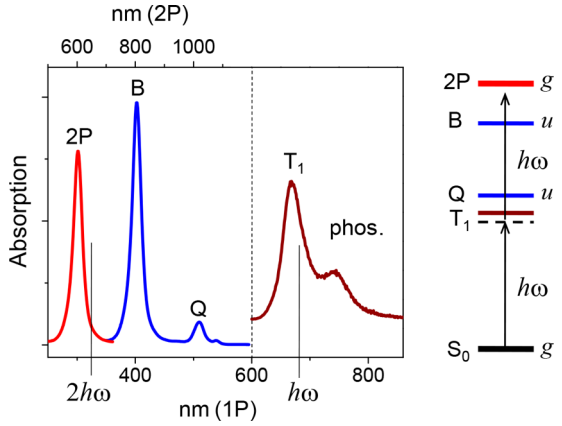

Figure 1. Experimental 1P absorption (blue) and phosphorescence (dark red) spectra of a typical Pt(II) porphyrin (e.g., Pt tetraarylporphyrin) and "predicted" 2P absorption (red) into a *g*-state. The energy diagram illustrating these processes is shown on the right.

porphyrins, the symmetry rules remain rather strong. The 2P-allowed *g*-states in porphyrins typically lie at much higher energy,[28−30] such that the excitation at half that energy overlaps with linear absorption into lower-lying 1P-allowed *u*-states (e.g., Q-state), fully overshadowing 2PA. In complexes of porphyrins with heavy metals, such as Pt and Pd, the situation is further exacerbated by strong spin−orbit coupling, which partially allows spin-forbidden absorption directly into the triplet state ($S_0 \rightarrow T_1$).[31,32] This linear process, although insignificant under normal light intensities, becomes the dominant absorption mechanism under excitation by high-intensity laser pulses, which are required to induce 2PA. As a result, it is the lowest triplet state (T_1) that effectively sets the upper limit for acceptable two-photon excitation energy in Pt and Pd porphyrins, and this energy is usually lower than required for excitation of the 2P-active *g*-states (Figure 1).

Various methods of enhancement of 2PA in tetrapyrroles have been explored over the years, including construction of expanded porphyrins, porphyrin oligomers and arrays,[5,15,18,33−36] adding polarizing substituents to create asymmetric dipolar push−pull-type[8,37−39] or symmetric quadrupolar systems,[12,16,19,40] and extending porphyrin π-system by way of asymmetric aromatic fusion,[41,42] as well as using indirect approaches based on 2PA antenna chromophores and subsequent energy transfer onto porphyrins.[17,20,43−46] In some cases, remarkably high 2PA cross sections have been achieved; however, triplet states in complex dye systems are frequently affected by undesirable quenching pathways (e.g., intramolecular charge transfer), which lead to a decrease or even complete loss of phosphorescence.[31] Furthermore, 2P-active porphyrin-based systems are usually large hydrophobic molecules, lacking intrinsic aqueous solubility and often exhibiting strong tendency to aggregate even in organic solutions. Good solubility, however, is critically important for many applications. For example, aggregation and/or non-specific hydrophobic interactions of optical probes with endogenous components of biological systems (proteins, nucleic acids, lipids etc.) may significantly affect biodistributions and/or perturb probes' function.

In a recent study we evaluated the effects of aromatic π-extension and peripheral substitution on 2PA properties of phosphorescent Pt(II) porphyrins.[47] Our key finding was that substitution of benzo-fused porphyrins with alkoxycarbonyl groups leads to strong stabilization of 2P-active *g*-states,

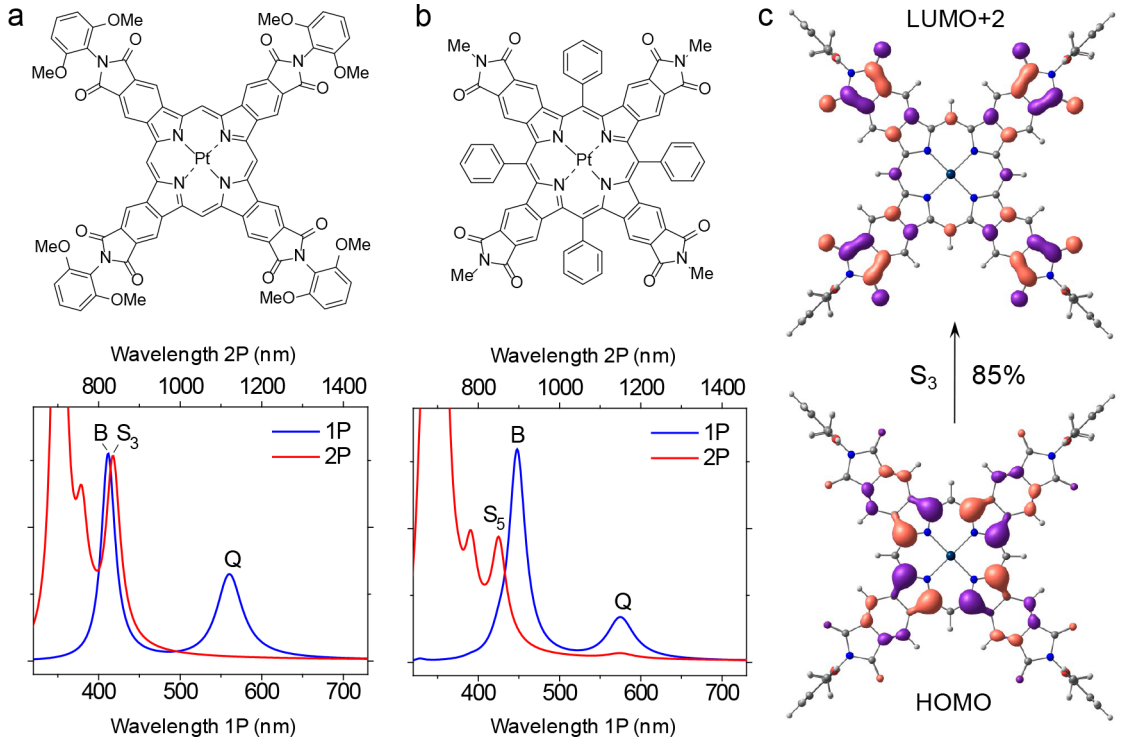

Figure 2. Structures and computed 1P and 2P absorption spectra of (a) Pt tetraarylphthalimidoporphyrin (PtTAPIP) and (b) Pt *meso*-tetraphenyltetramethylphthalimidoporphyrin ($PtPh_4TPIP$) and (c) Kohn−Sham orbitals participating in the leading term of the transition to the low-lying 2P active state S_3 in PtTAPIP. See Experimental Methods and Supporting Information for details of the computations.

DOI: 10.1021/acs.jpca.7b04333
J. Phys. Chem. A 2017, 121, 6243−6255

bringing them closer to the B-state level and thereby dramatically increasing 2PA near 800 nm. The origin of the stabilization could be traced back to the topology of the orbitals comprising the *g*-states, in which the electron density is pulled out of the macrocycle onto the adjacent carbonyl groups. Remarkably, the effect was found to be especially strong in fully symmetric (D_{4h}) *meso*-unsubstituted Pt octaalkoxycarbonyltetrabenzoporphyrins (PtTBP$(CO_2R)_8$, Figure 2), which are compact and easily accessible synthetically[48]—a benefit of the symmetrical structure—and possess very high phosphorescence quantum yields because of their rigidity and planarity.[47−49] Naturally, such combination of properties raised our interest in octacarbonyl-fused tetrabenzoporphyrins (TBP) as a potential platform for constructing probes for 2PLM and other applications, where strong 2PA, long triplet lifetime, manageable synthesis and relatively compact size are important criteria.

In the present study we first used TDDFT/SOS calculations to evaluate 2PA properties of several fully symmetric planar porphyrins amendable to synthetic modifications. The calculations predicted dramatic stabilization of strongly 2P-active *g*-states and consequently a major enhancement of 2PA in a *meso*-unsubstituted tetraphthalimidoporphyrin, which was expected to exhibit particularly high emissivity due to its nearly ideally planar structure. A scalable practical synthesis of this porphyrin was then developed, and spectroscopic and structural characterization fully confirmed predictions of the theory. Overall, the hand-in-hand combination of the theory and experiment proved to be an indispensible tool for understanding 2PA of phosphorescent porphyrins, helping to identify and design molecules for applications.

EXPERIMENTAL METHODS

General Information. The detailed description of the synthesis and characterization of all the compounds, including the details of X-ray crystal structure determination for compounds Zn-**7** and Pt-**11** can be found in the Supporting Information. Fluorescein, rhodamine 6G, and rhodamine B were obtained commercially and used as received. Solutions for optical measurements were prepared using spectroscopic grade methanol (MeOH), ethanol (EtOH) and dimethylacetamide (DMA). Quartz fluorometric cells were used in all optical experiments. All solutions of the phosphorescent porphyrins were rigorously deoxygenated using ultrapure argon (Airgas, grade 5) and/or by several freeze−degas−thaw cycles. Measurements of molar extinction coefficients, luminescence lifetimes and 2PA cross sections were performed as described in a recent publication[47] (also see the Supporting Information, p S3). For details of the emission quantum yield measurements, see the Supporting Information (p S3).

The quantum chemistry calculations were performed using in-house-modified Gaussian 09[50] in conjunction with M05-QX exchange-correlation functional.[51] The SDD Stuttgart effective core potentials were used for the metal atoms,[52] while D95 basis set[53] with no diffuse functions was used for all other elements in order to prevent artificial Rydberg contributions to the valence excited states.[54,55] For all porphyrins, 22 excited states were calculated using TDDFT. In all calculations the solvent effects were included using the dielectric continuum model in solvent model density (SMD) parametrization,[56] as implemented in Gaussian 09. For additional details see ref 47 and the Supporting Information (p S4).

RESULTS AND DISCUSSION

Structural and Spectroscopic Considerations. PtTBP−$(COX)_8$ and similar porphyrins (Chart 1a), where groups X are

Chart 1. Tetrabenzoporphyrins with Carbonyl-Containing Substituents in the Benzo Rings

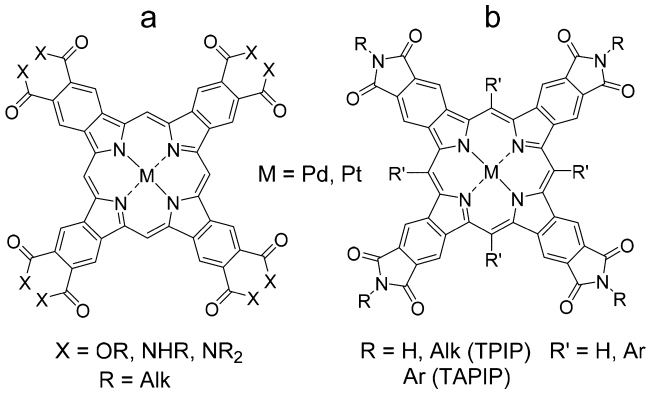

butoxy- or longer chain alkoxy- analogues (X = OR), are well-soluble in organic solvents (e.g., CH_2Cl_2, DMF) and show no traces of aggregation at concentrations required for optical measurements. However, to impart aqueous solubility the ester groups must be hydrolyzed and/or converted to some other functional groups (e.g., amides) with pendant hydrophilic residues. Unfortunately, the respective transformations proved to be remarkably inefficient due to the high propensity of TBP−octacarboxylic acids, as well as most of their amide derivatives (X = NHR), to aggregation. TBP−dialkylamides (X = NR_2), as expected, exhibit much better solubility; however, TBP−dialkylamides were found to be inferior to TBP−esters in terms of 2PA properties. One possible reason underlying this effect could be that in dialkylamides the carbonyl groups are rotated out of the porphyrin plane more than in esters, 60° vs 44° on average (Figure S1, p S16). As a result, the coupling between the carbonyls and the macrocycle, which apparently is essential for stabilization of 2P-active states,[47] is reduced, and the 2PA near the B-state is diminished. The specific details of these experiments and calculations will be reported elsewhere.

On the basis of the above results, we turned our attention to structures in which carbonyl groups are locked in plane with the TBP macrocycle. One such structure is the porphyrin extended by fusion of the pyrrolic rings with phthalimide residues (Chart 1b), i.e. tetraphthalimidoporphyrin. A synthesis of *meso*-tetraaryltetraalkylphthalimidoporphyrin (Ar_4TPIP) was recently published,[57] and a remarkably high phosphorescence quantum yield was reported for its Pt(II) complex. At the same time, the structure of the Ar_4TPIP molecule was reported to be highly nonplanar, which by analogy with tetrabenzoporphyrins implied that a *meso*-unsubstituted planar TPIP should be even more emissive.[49] Indeed, a reciprocal relationship between emissivity and nonplanarity is well-established across the porphyrin family.[49,58−61]

To evaluate the electronic effects of fused phthalimide residues and *meso*-aryl substitution on 2PA we carried out TDDFT/SOS calculations (see Experimental Methods and Supporting Information for details). The structures of the selected tetraphthalimidoporphyrins and their computed 1PA and 2PA spectra are shown in Figure 2. The data are summarized in Table 1, and the data for two additional

DOI: 10.1021/acs.jpca.7b04333
J. Phys. Chem. A 2017, 121, 6243−6255

Table 1. Calculated Energies, Oscillator Strengths, and 2PA Cross Sections of Model Tetraphthalimidoporphyrins (Figure 2)[a]

model compd	state	E singlets calcd (eV)[b]	λ calcd (nm)[c]	f calcd[d]	$\sigma^{(2)}$ calcd (GM)[e]
PtTAPIP	S_1, S_2 (Q)	2.21, 2.21	560, 560	0.60, 0.60	0.0, 0.0
	S_3 (2P)	2.97	418	0.00	518
	S_4, S_5 (B)	3.01, 3.01	412, 412	1.45, 1.45	0.0, 0.0
$PtPh_4TPIP$	S_1, S_2 (Q)	2.16, 2.16	575, 575	0.30, 0.30	7.0, 7.0
	S_3, S_4 (B)	2.77, 2.77	448, 448	1.47, 1.46	2.0, 2.0
	S_5 (2P)	2.91	425	0.21	289

[a]For complete data sets see Supporting Information (p S17). [b]Energies of singlet states S_n. Closely spaced states are grouped on the same line; only states relevant to the discussion are shown. [c]Wavelengths corresponding to 1P excitation. For 2P excitation these values should be doubled. [d]Oscillator strengths (for $S_0 \rightarrow S_n$). [e]2PA cross sections; 1 GM= 10^{-50} cm^4 s $molecule^{-1}$ $photon^{-1}$.

analogous porphyrins can be found in the Supporting Information (p S17).

meso-Unsubstituted tetraarylphthalimidoporphyrin (PtTAPIP, Figure 1a) was chosen because of its planarity and, therefore, potentially higher emissivity, as expected from the previously performed analysis of *meso*-unsubstituted tetrabenzoporphyrins.[47] We reasoned that it should be possible to prevent π-stacking and aggregation, while keeping the geometry of the macrocycle unperturbed, if the phthalimide nitrogens would be extended by 2,6-substituted aryl groups. The 2,6-substituted aryls should be forced to rotate out of the porphyrin plane by the steric effects, creating a barrier for face-to-face contacts between different porphyrin molecules. Indeed, calculations showed that 2,6-dialkoxydisubstituted aryl groups in PtTAPIP are tilted by ~70° relative to the macrocycle plane. In contrast, 3,5- or 4-substitited aryls can easily align with the porphyrin, potentially favoring rather than preventing formation of intermolecular stacks. At the same time, *N*-alkyl groups in the absence of *meso*-aryls are likely to produce only a small steric repulsion and therefore unlikely to prevent aggregation.

$PtPh_4TPIP$ (Figure 2b) was analyzed in view of the good solubility and favorable photophysical properties reported for its close analogue,[57] different only by alkyl substituents at the phthalimide nitrogens.

The most unusual feature predicted by the calculations was that in planar PtTAPIP (Figure 2a) a highly 2P-active *g*-state (S_3) is stabilized below the B-state level. Such low-lying *g*-states are rather unusual for porphyrins. For example, a similar *g*-state in PtTBP−octaester lies ~0.3 eV above the B-state,[47] however even in that case the experimentally measured 2PA near the B-state was already much higher than in regular symmetrical porphyrins. S_3 state in PtTAPIP involves predominantly one configuration: HOMO (a_{2u}) → LUMO+2 (b_{1u}), and just like in PtTBP−octaester the target orbital (LUMO+2) extends beyond the TBP macrocycle onto the adjacent carbonyls, while the HOMO is localized entirely within the tetrapyrrolic core (Figure 2c). Such shift of the electronic density from the core to the periphery appears to be a signature of 2P-active transitions in centrosymmetrical π-extended porphyrins. Similar patterns have been observed in porphyrins substituted *via meso*-positions with other electron withdrawing groups. For example, in recently reported diketopyrrolopyrrole−porphyrin arrays 2P-active states were calculated to possess similar core-to-periphery charge transfer character.[19]

Analysis of the 2P tensor for the excitation into the S_3 state in PtTAPIP (Supporting Information, p S23) and ref 47) shows that this transition occurs mainly through the Q-state pathway(s) ($S_0 \rightarrow Q_{x,y} \rightarrow S_3$), which account for ~51% of the total transition amplitude. The fraction of the pure B-state(s) pathway ($S_0 \rightarrow B_{x,y} \rightarrow S_3$) is only ~8%; however the interference pathways ($S_0 \rightarrow Q_{x,y} \rightarrow S_3|S_0 \rightarrow B_{x,y} \rightarrow S_3$) and their conjugates collectively contribute ~41% of the excitation. These numbers once again underscore the importance of the B-state for 2PA in porphyrins.[30,47]

In contrast to *meso*-unsubstituted porphyrins PtTAPIP and PtTPIP (p S18), $PtPh_4TPIP$ (Figure 2b) and $PtPh_4TAPIP$ (p S18) possess strongly saddled geometries, and their 2P-active states are located above the B states. This ordering could be a result of the strong stabilization of the B states themselves, which is known for nonplanar porphyrins.[49,58,61−63] A similar situation has been observed in the case of Ar_4TBP *vs meso*-unsubstituted TBP octaesters,[47] whereby the experimental 2PA cross sections of Ar_4TBP's near their B-states was much lower than in the case of *meso*-unsubstituted TBP's.

On the basis of the computational predictions and potentially good solubility and high emissivity of TAPIP, this porphyrin was chosen as our lead structure. *meso*-Tetraarylated analogues Ar_4TAPIP and Ar_4TPIP were synthesized as well in order to facilitate comparison between structures and spectroscopic properties.

Synthesis. Our synthetic approach to π-extended porphyrins is based on oxidative aromatization of porphyrins fused with nonaromatic rings.[48,64−67] Here we continued exploring this methodology, except that the order of reactions used to generate porphyrinogenic pyrrolic precursors, such as **5a** and **5b** (Scheme 1), was changed. Pyrrole **5a** was prepared via the Diels−Alder cycloaddition of 3-sulfoleno-pyrrole **4** and maleimide **3**. Alternative schemes, e.g., stepwise assembly of the pyrrole starting from a maleimide, converting it into the cyclohexeno-derivative, and further converting it into a substrate for the Barton−Zard reaction,[57] are significantly more laborious if one desires to have the flexibility in placing different substituents at the phthalimide nitrogens. The synthesis shown in Scheme 1 can be easily expanded on different pyrroles by simply reacting dienophiles (maleimides) with the single pyrrolic precursor **4**, while the multistep synthesis of this precursor has to be performed only once.

Synthesis of 3-sulfolene-pyrrole ester **4** was published previously;[68] however, characterization data and information about the reaction yield(s) could not be found. Here **4** was synthesized from 3-benzenesulfonyl-2,5-dihydrothiophene-1,1-dioxide[69] and *tert*-butylisocyanoacetate by the Barton-Zard method under optimized conditions. We found that the key to optimal yields are slow addition of reagents (during 4−5 h) and low reaction temperatures (−50 to −35 °C), which most likely help to minimize degradation of the target products.

Maleimide **3** was synthesized from 2-nitroresorcinol, which was alkylated with methyl- or ethyl-4-bromobutyrate into nitro-derivative **1** (86%) and subsequently reduced into aniline **2**

DOI: 10.1021/acs.jpca.7b04333
J. Phys. Chem. A 2017, 121, 6243−6255

Scheme 1. Synthesis of Pyrrolic Precursors 5a and 5b[a]

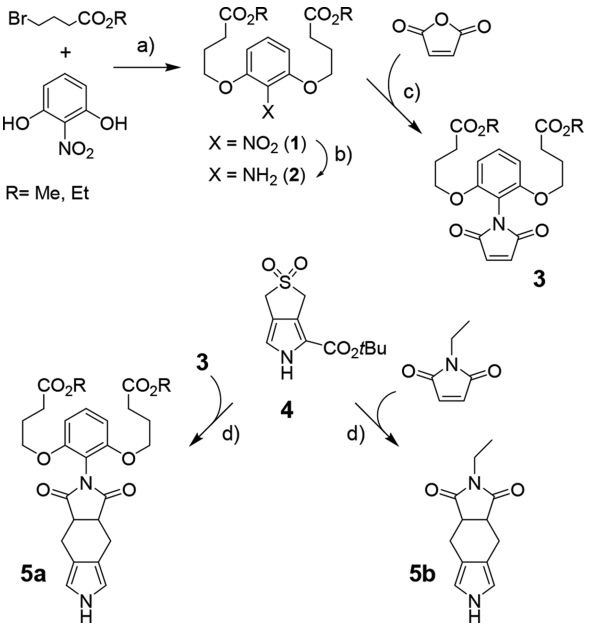

[a]Reagents and conditions: (a) K_2CO_3, DMF, 70 °C, 24 h (86%); (b) ammonium formate, THF/MeOH ~ 1:1, 10% Pd/C, reflux, 2 h (95%); (c) (i) TolH, room temperature, 2 h; (ii) NaOAc, Ac_2O, 100 °C, 2 h (82% over 2 steps); (d) 1,2,4-trichlorobenzene, reflux, 3 h (80–93%).

(10%). Here we used 4-bromobutyrates in order to introduce modifiable groups at the periphery of the target porphyrins (see below); however alkylation with other alkyl halides should be equally straightforward. Ethyl esters were found to be slightly advantageous vs methyl esters, as they rendered the target porphyrins more soluble in organic solvents.

Reaction of **2** with maleic anhydride, followed by the treatment of the intermediate with NaOAc in hot acetic anhydride, gave maleimide **3** in 82% yield. Remarkably, subsequent condensation of pyrrole-ester **4** with maleimide **3** led to the target pyrrole **5** in a single-pot reaction in 93% yield. Apparently, at high temperatures (reflux in trichlorobenzene) the Diels–Alder addition, *tert*-butyl ester cleavage, and decarboxylation occur simultaneously.

Condensation of pyrrole **5a** with formaldehyde (Scheme 2A) under the conditions developed previously for the synthesis of octaethylporphyrin (OEP)[70] led to porphyrinogens, which could be readily detected in the reaction mixtures by MALDI–TOF mass-spectrometry. The following conversion of the porphyrinogens into tetracyclohexeno-porphyrins **6** occurred upon purging the reaction mixtures with air. Free-base porphyrins H_2-**6** were isolated in 30–35% yields as mixtures of stereoisomers.

In order to facilitate aromatization of tetracyclohexenoporphyrins into tetraphthalimidoporphyrins the former were first metalated and subsequently oxidized (Scheme 2A, route 1).[48] Pt and Pd complexes were obtained in 80–85% yields upon refluxing of H_2-**6** with excess of the corresponding metal salts

Scheme 2. Synthesis of Tetraphthalimidoporphyrins[a]

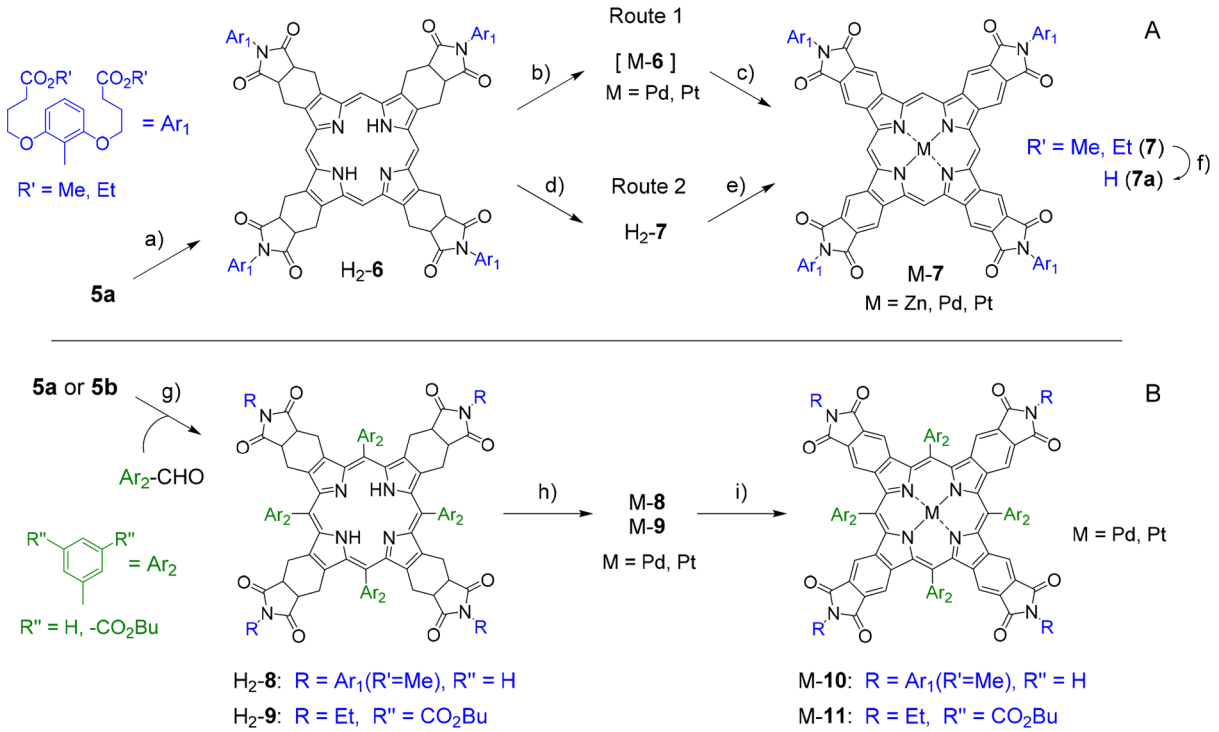

[a]Reagents and conditions for part A: (a) (i) CH_2O (aq, 37%), $TsOH{\cdot}H_2O$, toluene or benzene, Ar, reflux 8 h; (ii) air, room temperature, overnight (30–35%); route 1, (b) $Pt(acac)_2$, PhCN, reflux, 5–6 h (80%); or $Pd(OAc)_2$, PhCN, reflux, 20–30 min (80%) and (c) DDQ, ethyl benzoate, 130 °C, 4–5 h (70–75%); route 2, (d) DDQ, toluene, reflux, 48 h (50–60%) and (e) $Pt(acac)_2$, PhCN, reflux, 15–18 h (30–50%); or $Pd(OAc)_2$, PhCN, reflux, 2–3 h (30–50%); or $Zn(OAc)_2{\cdot}2H_2O$, THF:MeOH ~ 3:1, reflux, 2 h (70–80%); (f) AcOH/TFA/HCl ~ 1:0.5:1, room temperature, 24–48 h (95–100%). Reagents and conditions for part B: (g) (i) $BF_3{\cdot}Et_2O$, CH_2Cl_2, Ar, room temperature, 2 h; (ii) DDQ, room temperature, overnight; (h) $Pt(acac)_2$, PhCN, reflux, 2–4 h, or $Pd(OAc)_2$, PhCN, reflux, 20–30 min; (i) DDQ, toluene, reflux, 2–4 h. Yield: 14–20% over steps g–h.

DOI: 10.1021/acs.jpca.7b04333
J. Phys. Chem. A 2017, 121, 6243–6255

(acetylacetonates or acetates) in benzonitrile. Under these conditions partial oxidation of the cycloxeheno rings was observed (judged from the UV−vis spectra); however, isolation of pure Pt-**6** and Pd-**6** was not our goal, and therefore, these complexes were subjected to the final aromatization as crude mixtures.

Traditionally aromatization of cyclohexenoporphyrins into tetrabenzoporphyrins (and analogous syntheses of other π-extended porphyrins) is carried out in dioxane or toluene;[48,65] however, in the case of Pt-**6** and Pd-**6** these solvents were found to give rather poor results due to solubility issues. Instead, the aromatization was performed successfully in ethyl benzoate at 130 °C using excess 3,4-dichloro-5,6-dicyano-1,4-benzoquinone (DDQ), giving Pt-**7** and Pd-**7** in 70−80% yields.

An alternative route to metal derivatives of tetraphthalimidoporphyrins is to carry out oxidation of free-bases H_2-**6** first and then perform metalation (Scheme 2A, route 2). In this route, free-base tetraphthalimidoporphyrins H_2-**7** (R′ = Me, Et) were obtained in 50−60% yield upon refluxing of isolated pure H_2-**6** with DDQ in toluene for 48 h at high dilution, which was necessary to avoid aggregation of partially oxidized porphyrins. Free-bases H_2-**7** also could be obtained in 15−20% (methyl esters) or 30−35% (ethyl esters) yields by carrying out porphyrin condensation, followed by oxidation without isolation and purification of H_2-**6**. Insertion of Pt and Pd into H_2-**7** was accomplished in hot benzonitrile in 30−50% yields, however it was accompanied by formation of unidentified side products, likely of porphyrinic origin, which complicated purification of the target materials. Overall, oxidation after metalation (Scheme 2A, route 1) was found to be the preferred reaction order for Pt and Pd insertion. However, for insertion of Zn, route 2 turned out to be useful as well. Metalation of H_2-**7** using $Zn(OAc)_2$, which does not require high temperatures, occurred smoothly in MeOH/THF leading to pure Zn-**7** in 70−80% yield.

The synthesis of analogous *meso*-tetraaryl-substitiuted porphyrins **10** and **11** (Scheme 2B) in general followed a similar scheme. Porphyrin **10** has four *meso*-phenyl rings and the same 2,6-substututed aryl groups Ar_1 as its *meso*-unsubstituted analogue **7**. Porphyrin **11** resembles the previously synthesized *meso*-tetraarylphthalimidoporphyrin[57] by having *N*-alkyl substituents. In our case the alkyls were small ethyl groups, and in order to ensure solubility we used dibutoxycarbonyl *meso*-aryl substituents (Ar_2), which proved in the past to impart high solubility of various π-extended porphyrins.[47,48]

Pt and Pd complexes of **10** and **11** were synthesized in three steps from pyrrole **5a** (R′ = Me) and benzaldehyde (porphyrin **10**) or from pyrrole **5b** and 3,5-dibutoxycarbonylbenzaldehyde (porphyrin **11**) (Scheme 2B). Pyrrole **5b** was prepared by the Diels−Alder cycloaddition of sulfoleno-pyrrole **4** and commercial *N*-ethyl maleimide, demonstrating the versatility of **4** as a pyrrolic precursor. Cyclohexenoporphyrins H_2-**8** and H_2-**9** were prepared under the standard Lindsey conditions in the presence of $BF_3{\cdot}Et_2O$, followed by oxidation with DDQ. They were converted into the corresponding Pt or Pd complexes upon reflux with Pt or Pd salts (acetylacetonates or acetates) in benzonitrile. Finally, oxidation of M-**8** and M-**9** using DDQ in hot toluene yielded the target M-**10** and M-**11** (M = Pd, Pt) in 14−20% overall yields (for the three steps combined).

One of our goals was to develop porphyrins suitable for modification with hydrophilic substituents. It is for that reason the pendant groups in **7** were chosen to have ester functionalities, which after hydrolysis could be used in, e.g., amidation reactions. Unexpectedly, the hydrolysis of these phthalimidoporphyrin esters turned out to be not a straightforward task. Apparently, fusion of aryl- or alkylimido-fragments with tetrabenzoporphyrins makes these imides very sensitive to alkaline hydrolysis, much more so than the terminal ester functions. Breaking of the imides was observed under all conditions typically used in ester hydrolysis (e.g., LiOH in THF, $KOSiMe_3$ in DMF, LiI in pyridine, etc.). On the other hand, hydrolysis under strongly acidic conditions ($HCl_{conc.}$/TFA/HOAc) left imides completely intact while quantitatively giving octaacid Pt-**7a** (Scheme 2). Importantly for biological applications, the imide rings remained completely stable in aqueous solutions at pH ≤ 10.

The described above syntheses have been scaled up to obtain up to 0.5−0.6 g quantities of the final metalloporphyrins after a single run of the reaction sequence. To maintain optimal yields it is essential to keep the concentrations of the reaction mixtures as described in the experimental protocol.

Structures and Linear Photophysical Properties. The X-ray structures of two new tetraphthalimidoporphyrins, Zn-**7** (CCDC 1543009) and Pt-**10** (CCDC 1543010), are shown in Figure 3 along with the amplitudes of their dominant distortion

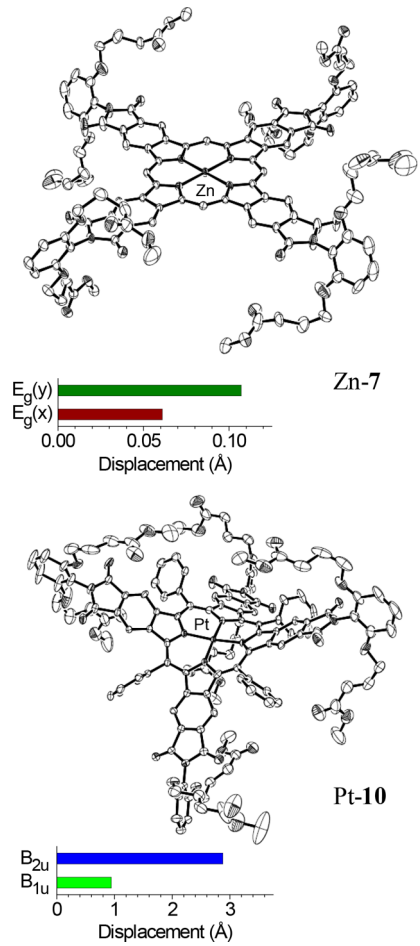

Figure 3. ORTEP views of the X-ray crystallographic structures of metalloporphyrins Zn-**7** and Pt-**10** (50% probability thermal ellipsoids). All hydrogen atoms and two coordinated pyridine molecules in Zn-**7** are omitted for clarity. The bar graphs show the magnitudes of the dominant out-of-plane distortion modes: *saddling* (B_{2u}), *ruffling* (B_{1u}) and *waving* ($E_g(x)$ and $E_g(y)$).

DOI: 10.1021/acs.jpca.7b04333
J. Phys. Chem. A 2017, 121, 6243−6255

Table 2. Selected Photophysical Properties of the Studied Metalloporphyrins[a]

compd	λ_{max} Q (nm)	λ_{max} B (nm)	E_{max} Q (eV)	E_{max} B (eV)	ϵ_{max} Q (M^{-1} cm^{-1})	ϵ_{max} B (M^{-1} cm^{-1})	f_{Q0}[b]	f_{B0}	λ_{max} emiss[c] (nm)	E_{max} T_1 (eV)	ϕ[d]	τ[e] (μs)	λ_{max} 2P[f] (nm)	E_{max} 2P[g] (eV)	$\sigma^{(2)}_{max}$ (GM)
Pt-7	616	433	2.01	2.86	274700	242500	0.80	1.91	744	1.67	0.45	49	900	2.75	616
Pd-7	629	444	1.97	2.79	263500	342900	0.71	1.93	769	1.61	0.23	450	905	2.74	594
									636[h]	–	0.012[h]				
Pt-**10**	635	467	1.95	2.65	147100	258800	0.48	1.63	761	1.63	0.048	8	915	2.71	222
Pd-**10**	650	481	1.91	2.58	144100	358900	0.46	1.82	794	1.56	0.004	14	925	2.68	143
Pt-**11**	639	463	1.94	2.68	152600	250800	0.56	1.80	774	1.60	0.12	23	910	2.72	262
Pd-**11**	653	476	1.90	2.60	137700	336900	0.49	1.80	808	1.53	0.008	31	920	2.69	142

[a]All measurements were performed in DMA at 22 °C. [b]*f*, oscillator strength. [c]"emiss", emission: in all cases, except that given in footnote *h*. $T_1 \rightarrow S_0$ phosphorescence. [d]ϕ - in all cases, except that given in footnote *h*, quantum yield of phosphorescence (ϕ_p). [e]τ, triplet state lifetime. [f]λ_{max} 2P, the wavelength corresponding to the 2PA peak. [g]Energy of the 2P-active state. [h]Thermally activated (E-type) delayed fluorescence. The emission quantum yields (ϕ) and lifetimes (τ) were measured in fully deoxygenated solutions.

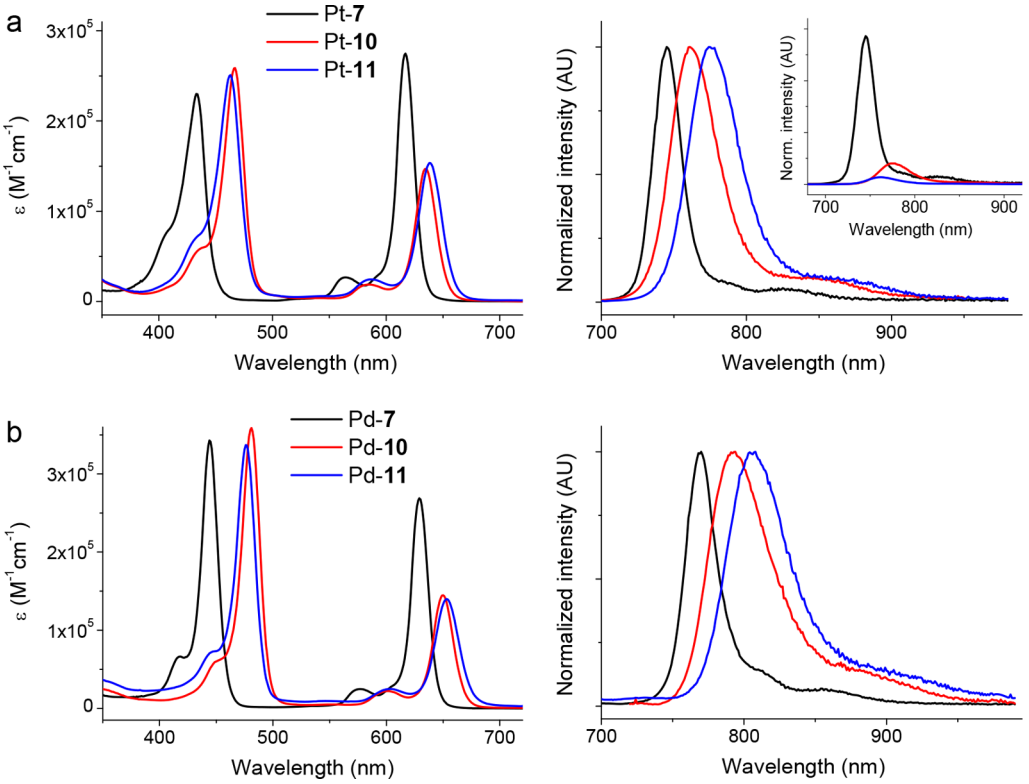

Figure 4. Absorption (left) and normalized phosphorescence (right) spectra of Pt (a) and Pd (b) tetraphthalimidoporphyrins **7** (R′ = Et), **10** (R′ = Et), and **11** in DMA at 22 °C. The inset shows phosphorescence spectra of the Pt complexes with integrated intensities scaled by the emission quantum yields. In the case of Pd complexes, the inset was omitted because the emission yields of Pd-**10** and Pd-**11** are very low.

modes as quantified by the normal mode structural decomposition (NSD) analysis.[71] Over the years NSD has proven to be avery useful tool for structural analysis of nonplanar porphyrins,[72−74] as it allows both classification and quantification of individual distortion types according to their symmetry.

To the best of our knowledge Zn-**7** is the first example of crystallographically characterized neutral complex of *meso*-unsubstituted π-extended porphyrin. Both visual inspection of the structures and the NSD plots clearly show that the macrocycle in Zn-**7** is nearly ideally planar, while Pt-**10** is strongly distorted. The dominant distortion mode in Pt-**10** is *saddling* (corresponding to the vibrational B_{2u} mode), and the total out-of-plane distortion amplitude (D_{oop}) is 3.03 Å, which is among the highest values known for metal complexes of tetraaryl-π-extended porphyrins.[57,75−80] In Zn-**7** the *saddling* (B_{2u}) and *ruffling* (B_{1u}) modes are virtually absent, but instead there are small *waving* distortions ($E_g(x)$ and $E_g(y)$). Their combined amplitudes, however, are an order of magnitude smaller than those in Pt-**10**. It is important to note that the central metal, whether it is Zn, Pd or Pt (but not Ni),[65] has only a minimal effect on the macrocycle structures, while the dominant distortion force is due to the interactions between the adjacent benzo- and *meso*-aryl groups. Therefore, it is reasonable to assume that the equilibrium structures of Pt and Pd complexes of *meso*-unsubstitited porphyrin **7** (Pt-**7** and Pd-**7**) should be as planar as that of Zn-**7** or of other structurally characterized *meso*-unsubstututed π-extended porphyrins.[81−83] Similarly, one can expect that **11** should be distorted as much as **10** (Figure S3, p S17). Indeed, an earlier published tetraaryltetraphthalimidoporphyrin was found to be saddled, although with somewhat lower total our-of-plane distortion (D_{oop} = 2.27 Å).[57]

DOI: 10.1021/acs.jpca.7b04333
J. Phys. Chem. A 2017, 121, 6243−6255

Previous studies have revealed reciprocal relationship between porphyrin planarity and emissivity.[49,58−61] Nonplanar distortions, in particular *saddling* and *ruffling*, are associated with higher flexibility of the macrocycle, and their presence correlates with enhancement of the low-frequency vibrations,[58,59,61] presumably in both ground and excited states. In the case of phosphorescent porphyrins these vibrations greatly enhance nonradiative triplet decay, leading to a dramatic loss of emissivity.[49] Although in aromatically π-extended porphyrins the effects of nonplanarity are significantly dampened compared to regular nonextended nonplanar porphyrins, saddled Pd and Pt *meso*-tetraaryltetrabenzo- and tetranaphthoporphyrins still possess much lower phosphorescence quantum yields than their planar counterparts.[48,84] In view of these earlier observations and considering the computed and experimental structures (Figure 3 and ref 57), one should expect Pt and Pd complexes of **7** to be much stronger emitters that those of **10** and **11**.

One important structural feature of Zn-**7** is that the N-aryl groups in this porphyrin are indeed tilted by ∼70° relative to the macrocycle plane. As a result, the substituents positioned in 2,6-positions of these rings are facing outward from the macrocycle, preventing intermolecular face-to-face contacts. This property was intentionally programmed into our design (see above), and it appeared to serve its purpose well. Porphyrins **7**, including the free-bases and metal complexes, are all well-soluble in organic solvents (CH_2Cl_2, THF, DMF, DMA, benzonitrile), showing no signs of formation of π-stacks and aggregation. As expected, nonplanar *meso*-tetraarylporphyrins **10** and **11** are also well-soluble at concentrations required for optical measurements.

The spectroscopic data for the new Pd and Pt porphyrins are summarized in Table 2, and the absorption and phosphorescence spectra are shown in Figure 4. Additional data can be found in the Supporting Information (Table S3, p S24). In the discussion below we focus only on the phosphorescent Pd and Pt complexes, however, fluorescent free-base and Zn porphyrins have also been isolated and characterized. The analytical and photophysical data for the free-base and Zn tetraphthalimidoporphyrins can be found in the Supporting Information.

Overall, the linear (1P) absorption spectra of the new tetraphthalimidoporphyrins reflect all the trends known for tetrabenzoporphyrins. First, nonplanar distortions due to the *meso*-aryl substitution, i.e., in **10** and **11** vs **7**, induce significant bathochromic shifts of both B and Q bands. This effect, characteristic of all nonplanar porphyrins,[63] is related to the partial engagement of the *meso*-aryl groups into the conjugation with the macrocycle, whereby the average dihedral angle between the mean-square plane drawn through the porphyrin and the *meso*-aryl rings is on the order of 30°.[85] Second, the spectra of Pd complexes are shifted bathochromically relative to those of Pt complexes, which is again a well-known trend for both regular and π-extended porphyrins.[86,87] Third, in planar complexes **7** the intensities of the Q bands are higher, especially in relation to the B bands, than in *meso*-tetraarylared analogues **10** and **11**.[47,48] For example, in Pt complexes the B/Q ratio of the oscillator strengths decreases from ∼3.3 to ∼2.4 in going from **10** or **11** to **7**, while the ratio of the peak intensities in Pt-**7** drops below one (0.88), owing to the exceptionally high molar extinction coefficient at the peak of the Q-band (ε_{616} = 274 700 M^{-1} cm^{-1}). For the Pd complex (Pd-**7**) the peak ε-value is also very high (263 500 M^{-1} cm^{-1}), and the Q-band absorption overlaps almost ideally with the excitation spectrum of a large family of red light-emitting diodes. From the practical perspective this is a very useful feature in view of potential applications of Pt and Pd complexes as imaging probes.[80]

The spectral bands of the porphyrins containing aryl units at the phthalimide nitrogens (**10**) are slightly shifted relative to those of *N*-alkyl-substituted porphyrins (**11**), indicating presence of weak electronic coupling between the N-aryls and the macrocycle system. These N-substituents, positioned at rather remote ends of the macrocycle, apparently have much stronger influence on the triplet decay properties than on the bands energies (see below).

Heavy Pd and Pt atoms induce strong spin orbit coupling in **7**, **10**, and **11**. Upon excitation these molecules undergo $S_1 \rightarrow T_1$ intersystem crossing nearly instantaneously. The triplet states in all cases decay with emission of phosphorescence, however the emission properties are significantly different between the porphyrins. Pt complexes are generally brighter and have higher rates constants of both radiative (k_r) and nonradiate (k_{nr}) decays, as expected from the presence of the heavier element (Pt) and, therefore, stronger spin−orbit coupling. Both k_r and k_{nr} decrease in Pd complexes (Table S3, p S24), but so does the k_r/k_{nr} ratio, resulting on average in substantially lower phosphorescent quantum yields. However, Pd-**7** is still strongly emissive (ϕ_p = 0.23), and the very long lifetime of its triplet state (τ = 450 μs) is clearly beneficial for applications of phosphorescence quenching where high resolution in the determination of quencher concentrations is required, such as in some biological oxygen sensing experiments.[88,89]

In addition to phosphorescence Pd-**7** exhibits pronounced thermally activated delayed (E-type) fluorescence, which has its maximum near 636 nm and the quantum yield of $\phi_{fl}(d)$ = 0.012 at 22 °C in deoxygenated DMA (Figure S6, p S25). Upon pulsed excitation the fluorescence signal decays with the same time constant (τ = 450 μs) as the phosphorescence, and upon contact with air its intensity decreases proportional to the phosphorescence as well. In contrast, in fully aerated solutions, where the intensity of phosphorescence drops by more than 700 times, the fluorescence decreases only by ∼32 times. The small remaining signal ($\phi \sim 0.0004$) is likely be due to the residual prompt fluorescence.

Because of its excellent spectral separation from the phosphorescence, the delayed fluorescence provides means for ratiometric time-resolved sensing of temperature—a unique feature that should be explored in future studies. Indeed, the ratio of the delayed fluorescence vs phosphorescence for Pd-**7** in DMA increases almost two times (from 0.067 to 0.12) in going from 22 to 40 °C (Figure S7, p S25). In the case of Pt-**7**, the delayed fluorescence signal, although detectable in principle, is too weak to allow quantification and/or to be of practical significance.

As expected from the known structure−property relationships, the emissivity of the nonplanar porphyrins **10** and **11** overall is markedly lower compared to that of the flat and more rigid porphyrin **7**. The phosphorescence quantum yield of Pt-**7** in solution at 22 °C is 0.45, making this molecule one of the brightest phosphorescent emitters known today. The decrease in the emission quantum yields in nonplanar complexes is due to the higher rates of the nonradiative triplet decays (Table S3, p S24). However, just like in the related tetrabenzoporphyrins nonplanar distortions do not completely quench phosphorescence,[49,62] but only decrease it by several fold. Therefore, Pt-

DOI: 10.1021/acs.jpca.7b04333
J. Phys. Chem. A 2017, 121, 6243−6255

10 and Pt-**11** still retain emissivity, although in Pd complexes the nonradiative decay strongly outcompetes emission.

It is important to note that the phosphorescence quantum yield of Pt-**11** in deoxygenated toluene at 22 °C (Table S4, p S26) was determined in this work to be $\phi_p = 0.15$ ($\tau = 22$ μs), that is three times lower than the quantum yield reported for the analogous Pt tetaaryltetraphthalimidoporphyrin ($\phi_p = 0.45$, $\tau = 14$ μs) under identical conditions.[57] The latter molecule was different only by the alkyl groups at the phthalimide nitrogens and the substituents in the *meso*-aryl rings. On the basis of our previous studies,[80,84] it seems rather unlikely that the butoxycarbonyl groups in the *meso*-aryls of Pt-**11**, as compared to unsubstituted phenyls in the porphyrin from ref 57, could influence the emissivity significantly. Indeed, the emission quantum yield of $PtAr_4TBP$ (Ar = 3,5-$(BuCO_2)_2C_6H_3$) was determined in this work to be 0.20 vs 0.24 for Pt tetraphenyltetrabenzoporphyrin ($PtPh_4TBP$) (Table S4, p S26). It is equally improbable that the change of *N*-alkyl groups from isooctyls in the previous molecule[57] to ethyls in Pt-**11** would have a pronounced effect on the phosphorescence. The discrepancy most likely stems from the use of different actinometers and/or, possibly miscalibrated instrumentation. Indeed, in ref 57 the actinometer was $PtPh_4TBP$, whose phosphorescence quantum yield was considered to be 0.35, based on previous reports.[62,90] In our hands, however, the phosphorescence quantum yield of $PtPh_4TBP$ (measured in toluene at 22 °C) was found to be 0.24. If the emission quantum yield of $PtPh_4TBP$ were indeed close to 0.35, then *meso*-unsubstituted porphyrin Pt-**7**, measured in the same setup under the same conditions, would have the phosphorescence quantum yield of 0.66, which is an unlikely high value. On the other hand, the value of 0.45 for Pt-**7** determined here is in good agreement with other measurements performed on planar tetrabenzoporphyrins.[47,91] This suggests that the values of 0.35 for $PtPh_4TBP$ and 0.45 for the analogue of Pt-**11** reported in ref 57 are indeed exaggerated.

The transition from *N*-alkyl to N-aryl substituents in porphyrins **11** vs **10** leads to a significant drop in emissivity. This effect is largely due to the enhancement of the nonradiative triplet decay, whose rate increases 3-fold in going from, e.g., Pt-**11** to Pt-**10**, while the corresponding radiative rate practically does not change. The change in the triplet energy alone between complexes of Pt-**11** and Pt-**10**, which in principle could explain lower phosphorescence of Pt-**11** in view of the energy gap law,[92] is probably too small (~0.03 eV) to play a significant role. Therefore, other mechanisms, possibly associated with the dynamics of the flexible molecule **11** on the T_1 energy surface, containing geometries in which the spin−orbit coupling is much more enhanced than in **10**, are responsible for higher rate of $T_1 \rightarrow S_0$ intersystem crossing.

2PA Properties. The 2PA spectra of Pt complexes of porphyrins **7**, **10**, and **11** are shown in Figure 5. Similar spectra of Pd complexes can be found in the Supporting Information (Figure S8, p S27). All the 2PA measurements were performed by the 2P phosphorescence excitation method, using the setup described previously.[47] In brief, deoxygenated solutions of known concentrations were excited by short trains (1−2 μs) of ultrafast pulses from a tunable Ti:sapphire oscillator, gated by a Pockels cell. The resulting decays of phosphorescence were integrated, corrected and referenced against the signal of a standard with known 2PA cross section. Such measurements were performed at each excitation wavelength, typically stepping over the entire tunability range of the laser with ca.

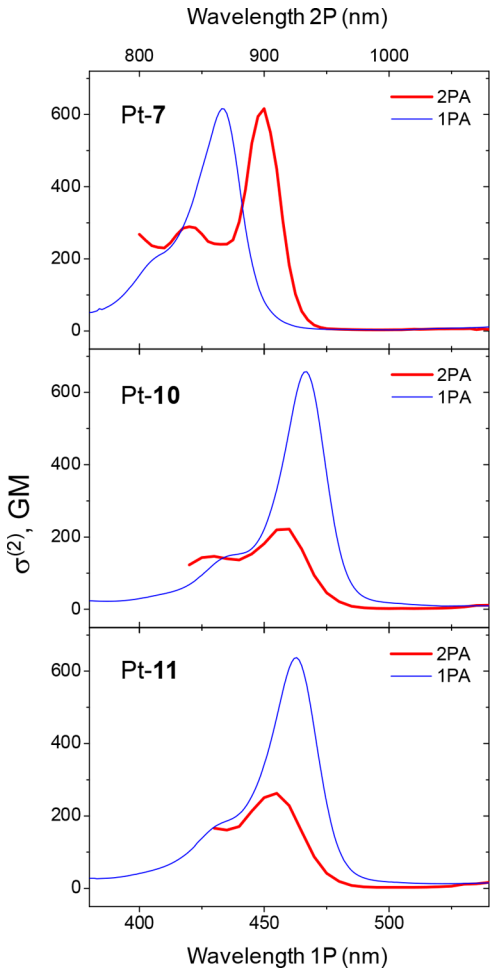

Figure 5. 2PA and 1PA spectra of Pt porphyrins in the B band region (measured in DMA at 22 °C). The 1PA spectra of the porphyrins are scaled to retain the relative intensities of the B bands.

5 nm step. In this work we probed the absorption in the B state region, using a laser with the tuning range of 680−1080 nm (Chameleon Ultra II, Coherent). At each excitation wavelength shown in the plots in Figure 5, 2PA was confirmed to be the dominant absorption mechanism: the log−log plots of the power dependencies had the slope of 2.00 ± 0.05. At the wavelengths shorter than ~820 nm (depending on the porphyrin) the spectra were truncated, since at higher energies direct 1P excitation into the triplet state (see Figure 1 and the accompanying text) became a strongly interfering linear excitation pathway.

The most notable feature seen in Figure 5 and Figure S8 (p S27) is that in both Pt-7 and Pd-7 sharp 2PA bands occur at the wavelengths longer than those corresponding to the B band transitions, which agrees precisely with predictions of the theory (Figure 2 and Table 1). As mentioned above, such substantial stabilization of *g*-states in tetrapyrroles is rather uncommon, although some examples of 2PA below the B state can be found in the literature.[12,19] In these examples, however, the whole tetrapyrrole electronic structure (i.e., two distinct states, Q and B, in the visible region[28]) of the molecule was perturbed, while in compounds **7** the 1P spectral shapes common for tetrabenzoporphyins are fully conserved, and only the *g*-states are affected by the substitution. It is also remarkable that the 2P-active states in **7** are completely invisible in the 1PA

DOI: 10.1021/acs.jpca.7b04333
J. Phys. Chem. A 2017, 121, 6243−6255

spectra, showcasing the symmetry selection rules and implying that in these rigid centrosymmetric molecules asymmetric vibrations, which could in principle partially allow these transitions, are weak.

The 2PA maxima of the tetraaryl-derivatives Pt-**10** and Pt-**11** are positioned higher in energy than the B absorption peaks, again in full agreement with predictions of the theory. The 2P peaks in **10** and **11** are red-shifted by ∼0.03 eV compared to **7**, however the shifts of the B bands (and Q bands as well) themselves are larger (∼0.06 eV). These relative changes in energies upon *meso*-tetraarylation are ultimately responsible for the ordering or the states, and the same effect was observed in earlier ester-substituted tetrabenzoporphyrins.[47]

The peak values of the 2PA cross sections of Pd-**7** and Pt-**7** are on the order of 600 GM, making these porphyrins the brightest two-photon absorbing phosphorescent emitters known today. From the practical perspective, efficient 2PA near 900 nm and emission bands near 770 nm are an excellent combination of properties, which should allow deeper tissue sampling in imaging applications such as 2PLM and efficient localized generation of singlet oxygen in 2P PDT.

The 2PA cross section values of complexes of **10** and **11**, again rather accurately predicted by the calculations, are on average ∼2.5 times lower than those of **7**. Although these values are still quite high compared to other symmetric porphyrins, the relatively low emission yields of **10** and **11** make them inferior to *meso*-unsubstituted porphyrins **7**. Thus, the two-photon brightness (the product of the absorption cross section and emission quantum yield) even of the brightest *meso*-tetraarylated complex Pt-**11** is almost 10 times lower than that of the *meso*-unsubstituted counterpart Pt-**7**.

In all cases the computed states' energies (Table 1) are somewhat higher than those measured experimentally (Table 2), similar to what we have encountered in our earlier calculations of π-extended porphyrins.[47] This is in part due to the fact that computations render vertical unrelaxed excitation energies and in part is a general property of DFT. While TDDFT tends to underestimate excitation energies for polyenes,[93] it overestimates them for cyanines[94,95,95] and to a lesser extent for porphyrins. The reasons for these effects have been investigated and solutions have been proposed.[94,96] In the future it may be desirable to develop functionals optimized specifically for porphyrins, capable of more accurate predictions of their 1P and 2P spectra. Nevertheless, even in the present form, the calculations overall were able to accurately reproduce the trends and helped identify new practically useful porphyrinoids, whose key spectroscopic properties (e.g., 2PA) could not be easily measured experimentally.

CONCLUSIONS

In this work we used the quantum chemistry and structure–property relationships-guided design to identify porphyrinoids with characteristics optimal for applications relying on two-photon excitation and subsequent generation of phosphorescent triplet states. It is important to emphasize that the calculations in the present study served not only to rationalize the experimentally observed spectroscopic properties but also to predict the optical spectra of rather complex metalloporphyrin structures prior to their synthesis and experimental evaluation. A general and efficient synthetic strategy leading to the identified structures has then been developed, and the resulting compounds proved to possess the predicted properties.

The synthetic strategy based on sulfolenopyrroles is a useful addition to the toolkit of porphyrin chemistry. For example, when combined with the oxidative aromatization method it expands and simplifies approach to a number of π-extended porphyrins fused with exocyclic rings. The newly synthesized Pt and Pd *meso*-unsubstituted tetraphthalimidoporphyrins are exceptionally bright phosphorescent chromophores, which are expected to give rise to the next generation of imaging probes and possibly novel drugs for targeted photodynamic therapy. Furthermore, the combination of thermally activated delayed fluorescence and phosphorescence in the Pd complex may lead to probes for time-resolved imaging of temperature. The corresponding work is currently underway.

Lastly, it is worth noting that near-infrared phosphorescence of the new porphyrins is likely to attract interest in material science applications, such as in construction of organic light emitting diodes (OLED) and other areas concerned with efficient triplet generation and emission. Synthetic accessibility of the new chromophores should facilitate the respective studies.

ASSOCIATED CONTENT

Supporting Information

The Supporting Information is available free of charge on the ACS Publications website at DOI: 10.1021/acs.jpca.7b04333.

Additional experimental details, optical spectroscopic data, and results of calculations (PDF)

AUTHOR INFORMATION

Corresponding Author

*(S.A.V.) E-mail: vinograd@mail.med.upenn.edu.

ORCID

Héctor J. Rivera-Jacquez: 0000-0003-3787-5479

Artëm E. Masunov: 0000-0003-4924-3380

Sergei A. Vinogradov: 0000-0002-4649-5534

Notes

The authors declare no competing financial interest.

ACKNOWLEDGMENTS

Support of Grants EB018464 and NS092986 from the National Institutes of Health (S.A.V.), from the US National Science Foundation through the Penn MRSEC DMR11-20901 and its optical microscopy program (S.A.V.), from the Swiss National Science Foundation (B.W.) and from the Government of the Russian Federation (Act 211, Contract No. 02.A03.21.0011) (A.E.M.) is gratefully acknowledged. Computations were performed in part at the National Energy Research Scientific Computing Center (NERSC) and at the Advanced Research Computing Center (https://arcc.ist.ucf.edu) of the University of Central Florida. B.W. is a member of the Clinical Research Priority Program "Molecular Imaging Network Zurich". The authors are grateful to Dr. Patrick Carrol (Department of Chemistry, University of Pennsylvania) for X-ray structure determination.

REFERENCES

(1) Khurana, M.; Collins, H. A.; Karotki, A.; Anderson, H. L.; Cramb, D. T.; Wilson, B. C. Quantitative in vitro demonstration of two-photon photodynamic therapy using Photofrin(R) and Visudyne(R). *Photochem. Photobiol.* **2007**, *83*, 1441.

(2) Collins, H. A.; Khurana, M.; Moriyama, E. H.; Mariampillai, A.; Dahlstedt, E.; Balaz, M.; Kuimova, M. K.; Drobizhev, M.; Yang, V. X.

DOI: 10.1021/acs.jpca.7b04333
J. Phys. Chem. A 2017, 121, 6243–6255

D.; Phillips, D.; et al. Blood-vessel closure using photosensitizers engineered for two-photon excitation. *Nat. Photonics* **2008**, *2*, 420.
(3) Abrahamse, H.; Hamblin, M. R. New photosensitizers for photodynamic therapy. *Biochem. J.* **2016**, *473*, 347.
(4) Scherer, K. M.; Bisby, R. H.; Botchway, S. W.; Parker, A. W. New approaches to photodynamic therapy from Types I, II and III to Type IV using one or more photons. *Anti-Cancer Agents Med. Chem.* **2017**, *17*, 171.
(5) Kim, K. S.; Lim, J. M.; Osuka, A.; Kim, D. Various strategies for highly-efficient two-photon absorption in porphyrin arrays. *J. Photochem. Photobiol., C* **2008**, *9*, 13.
(6) Pawlicki, M.; Collins, H. A.; Denning, R. G.; Anderson, H. L. Two-photon absorption and the design of two-photon dyes. *Angew. Chem., Int. Ed.* **2009**, *48*, 3244.
(7) Aratani, N.; Kim, D.; Osuka, A. π-Conjugation enlargement toward the creation of multi-porphyrinic systems with large two-photon absorption properties. *Chem. - Asian J.* **2009**, *4*, 1172.
(8) Collini, E.; Mazzucato, S.; Zerbetto, M.; Ferrante, C.; Bozio, R.; Pizzotti, M.; Tessore, F.; Ugo, R. Large two photon absorption cross section of asymmetric Zn(II) porphyrin complexes substituted in the meso or beta pyrrolic position by -CC-C_6H_4X moieties(X = NMe_2, NO_2). *Chem. Phys. Lett.* **2008**, *454*, 70.
(9) Morisue, M.; Ogawa, K.; Kamada, K.; Ohta, K.; Kobuke, Y. Strong two-photon and three-photon absorptions in the antiparallel dimer of a porphyrin-phthalocyanine tandem. *Chem. Commun.* **2010**, *46*, 2121.
(10) Kamada, K.; Hara, C.; Ogawa, K.; Ohta, K.; Kobuke, Y. Strong two-photon absorption and its saturation of a self-organized dimer of an ethynylene-linked porphyrin tandem. *Chem. Commun.* **2012**, *48*, 7988.
(11) Pawlicki, M.; Morisue, M.; Davis, N. K. S.; McLean, D. G.; Haley, J. E.; Beuerman, E.; Drobizhev, M.; Rebane, A.; Thompson, A. L.; Pascu, S. I.; et al. Engineering conjugation in para-phenylene-bridged porphyrin tapes. *Chemical Sci.* **2012**, *3*, 1541.
(12) Nowak-Krol, A.; Wilson, C. J.; Drobizhev, M.; Kondratuk, D. V.; Rebane, A.; Anderson, H. L.; Gryko, D. T. Amplified Two-Photon Absorption in Trans-A_2B_2-Porphyrins Bearing Nitrophenylethynyl Substituents. *ChemPhysChem* **2012**, *13*, 3966.
(13) Nowak-Krol, A.; Grzybowski, M.; Romiszewski, J.; Drobizhev, M.; Wicks, G.; Chotkowski, M.; Rebane, A.; Gorecka, E.; Gryko, D. T. Strong two-photon absorption enhancement in a unique bis-porphyrin bearing a diketopyrrolopyrrole unit. *Chem. Commun.* **2013**, *49*, 8368.
(14) Mongin, O.; Sankar, M.; Charlot, M.; Mir, Y.; Blanchard-Desce, M. Strong enhancement of two-photon absorption properties in synergic 'semi-disconnected' multiporphyrin assemblies designed for combined imaging and photodynamic therapy. *Tetrahedron Lett.* **2013**, *54*, 6474.
(15) Varnavski, O.; Raymond, J. E.; Yoon, Z. S.; Yotsutuji, T.; Ogawa, K.; Kobuke, Y.; Goodson, T., III Compact self-assembled porphyrin macrocycle: synthesis, cooperative enhancement and ultrafast response. *J. Phys. Chem. C* **2014**, *118*, 28474.
(16) Schmitt, J.; Heitz, V.; Sour, A.; Bolze, F.; Ftouni, H.; Nicoud, J.-F.; Flamigni, L.; Ventura, B. Diketopyrrolopyrrole-porphyrin conjugates with high two-photon absorption and singlet oxygen generation for two-photon photodynamic therapy. *Angew. Chem., Int. Ed.* **2015**, *54*, 169.
(17) Mongin, O.; Hugues, V.; Blanchard-Desce, M.; Merhi, A.; Drouet, S.; Yao, D.; Paul-Roth, C. Fluorenyl porphyrins for combined two-photon excited fluorescence and photosensitization. *Chem. Phys. Lett.* **2015**, *625*, 151.
(18) Mikhaylov, A.; Kondratuk, D. V.; Cnossen, A.; Anderson, H. L.; Drobizhev, M.; Rebane, A. Cooperative enhancement of two-photon absorption in self-assembled Zinc-porphyrin nanostructures. *J. Phys. Chem. C* **2016**, *120*, 11663.
(19) Alam, M. M.; Bolze, F.; Daniel, C.; Flamigni, L.; Gourlaouen, C.; Heitz, V.; Jenni, S.; Schmitt, J.; Sour, A.; Ventura, B. π-Extended diketopyrrolopyrrole-porphyrin arrays: one- and two-photon photophysical investigations and theoretical studies. *Phys. Chem. Chem. Phys.* **2016**, *18*, 21954.
(20) Finikova, O. S.; Lebedev, A. Y.; Aprelev, A.; Troxler, T.; Gao, F.; Garnacho, C.; Muro, S.; Hochstrasser, R. M.; Vinogradov, S. A. Oxygen microscopy by two-photon-excited phosphorescence. *ChemPhysChem* **2008**, *9*, 1673.
(21) Sakadzic, S.; Roussakis, E.; Yaseen, M. A.; Mandeville, E. T.; Srinivasan, V. J.; Arai, K.; Ruvinskaya, S.; Devor, A.; Lo, E. H.; Vinogradov, S. A.; et al. Two-photon high-resolution measurement of partial pressure of oxygen in cerebral vasculature and tissue. *Nat. Methods* **2010**, *7*, 755.
(22) Lecoq, J.; Parpaleix, A.; Roussakis, E.; Ducros, M.; Houssen, Y. G.; Vinogradov, S. A.; Charpak, S. Simultaneous two-photon imaging of oxygen and blood flow in deep cerebral vessels. *Nat. Med.* **2011**, *17*, 893.
(23) Devor, A.; Sakadzic, S.; Saisan, P. A.; Yaseen, M. A.; Roussakis, E.; Srinivasan, V. J.; Vinogradov, S. A.; Rosen, B. R.; Buxton, R. B.; Dale, A. M.; et al. "Overshoot" of O_2 is required to maintain baseline tissue oxygenation at locations distal to blood vessels. *J. Neurosci.* **2011**, *31*, 13676.
(24) Kazmi, S. M. S.; Salvaggio, A. J.; Estrada, A. D.; Hemati, M. A.; Shaydyuk, N. K.; Roussakis, E.; Jones, T. A.; Vinogradov, S. A.; Dunn, A. K. Three-dimensional mapping of oxygen tension in cortical arterioles before and after occlusion. *Biomed. Opt. Express* **2013**, *4*, 1061.
(25) Parpaleix, A.; Houssen, Y. G.; Charpak, S. Imaging local neuronal activity by monitoring pO_2 transients in capillaries. *Nat. Med.* **2013**, *19*, 241.
(26) Spencer, J. A.; Ferraro, F.; Roussakis, E.; Klein, A.; Wu, J. W.; Runnels, J. M.; Zaher, W.; Mortensen, L. J.; Alt, C.; Turcotte, R.; et al. Direct measurement of local oxygen concentration in the bone marrow of live animals. *Nature* **2014**, *508*, 269.
(27) Lyons, D. G.; Parpaleix, A.; Roche, M.; Charpak, S. Mapping oxygen concentration in the awake mouse brain. *eLife* **2016**, *5*, 12024.
(28) Gouterman, M. Spectra of porphyrins. *J. Mol. Spectrosc.* **1961**, *6*, 138.
(29) Masthay, M. B.; Findsen, L. A.; Pierce, B. M.; Bocian, D. F.; Lindsey, J. S.; Birge, R. R. A theoretical investigation of the one-photon and two-photon properties of porphyrins. *J. Chem. Phys.* **1986**, *84*, 3901.
(30) Greco, J. A.; Shima, S.; Wagner, N. L.; McCarthy, J. R.; Atticks, K.; Brueckner, C.; Birge, R. R. Two-photon spectroscopy of the Q-bands of *meso*-tetraphenyl-porphyrin and chlorin framework derivatives. *J. Phys. Chem. C* **2015**, *119*, 3711.
(31) Finikova, O. S.; Troxler, T.; Senes, A.; DeGrado, W. F.; Hochstrasser, R. M.; Vinogradov, S. A. Energy and electron transfer in enhanced two-photon-absorbing systems with triplet cores. *J. Phys. Chem. A* **2007**, *111*, 6977.
(32) Knyukshto, V. N.; Shul'ga, A. M.; Sagun, E. I.; Zen'kevich, E. I. Formation of intersystem crossing transitions in Pd(II) and Pt(II) porphyrins: Nonplanar distortions of the macrocycle and charge transfer states. *Opt. Spectrosc.* **2006**, *100*, 590.
(33) Kurotobi, K.; Kim, K. S.; Noh, S. B.; Kim, D.; Osuka, A. A quadruply azulene-fused porphyrin with intense near-IR absorption and a large two-photon absorption cross section. *Angew. Chem., Int. Ed.* **2006**, *45*, 3944.
(34) Ikeda, C.; Yoon, Z. S.; Park, M.; Inoue, H.; Kim, D.; Osuka, A. Helicity induction and two-photon absorbance enhancement in zinc(II) meso-meso linked porphyrin oligomers via intermolecular hydrogen bonding interactions. *J. Am. Chem. Soc.* **2005**, *127*, 534.
(35) Yoon, Z. S.; Kwon, J. H.; Yoon, M. C.; Koh, M. K.; Noh, S. B.; Sessler, J. L.; Lee, J. T.; Seidel, D.; Aguilar, A.; Shimizu, S.; et al. Nonlinear optical properties and excited-state dynamics of highly symmetric expanded porphyrins. *J. Am. Chem. Soc.* **2006**, *128*, 14128.
(36) Ahn, T. K.; Kwon, J. H.; Kim, D. Y.; Cho, D. W.; Jeong, D. H.; Kim, S. K.; Suzuki, M.; Shimizu, S.; Osuka, A.; Kim, D. Comparative photophysics of [26]- and [28]hexaphyrins(1.1.1.1.1.1): Large two-photon absorption cross section of aromatic [26]-hexaphyrins(1.1.1.1.1.1). *J. Am. Chem. Soc.* **2005**, *127*, 12856.
(37) Karotki, A.; Drobizhev, M.; Kruk, M.; Spangler, C.; Nickel, E.; Mamardashvili, N.; Rebane, A. Enhancement of two-photon

DOI: 10.1021/acs.jpca.7b04333
J. Phys. Chem. A 2017, 121, 6243−6255

absorption in tetrapyrrolic compounds. *J. Opt. Soc. Am. B* **2003**, *20*, 321.
(38) Drobizhev, M.; Meng, F. Q.; Rebane, A.; Stepanenko, Y.; Nickel, E.; Spangler, C. W. Strong two-photon absorption in new asymmetrically substituted porphyrins: Interference between charge-transfer and intermediate-resonance pathways. *J. Phys. Chem. B* **2006**, *110*, 9802.
(39) Chandra Jha, P.; Minaev, B.; Agren, H. One- and two-photon absorptions in asymmetrically substituted free-base porphyrins: A density functional theory study. *J. Chem. Phys.* **2008**, *128*, 074302.
(40) Drobizhev, M.; Karotki, A.; Kruk, M.; Mamardashvili, N. Z.; Rebane, A. Drastic enhancement of two-photon absorption in porphyrins associated with symmetrical electron-accepting substitution. *Chem. Phys. Lett.* **2002**, *361*, 504.
(41) Makarov, N. S.; Drobizhev, M.; Wicks, G.; Makarova, E. A.; Lukyanets, E. A.; Rebane, A. Alternative selection rules for one- and two-photon transitions in tribenzotetraazachlorin: Quasi-centrosymmetrical pi-conjugation pathway of formally non-centrosymmetrical molecule. *J. Chem. Phys.* **2013**, *138*, 214314.
(42) Esipova, T. V.; Vinogradov, S. A. Synthesis of phosphorescent asymmetrically π-extended porphyrins for two-photon applications. *J. Org. Chem.* **2014**, *79*, 8812.
(43) Brinas, R. P.; Troxler, T.; Hochstrasser, R. M.; Vinogradov, S. A. Phosphorescent oxygen sensor with dendritic protection and two-photon absorbing antenna. *J. Am. Chem. Soc.* **2005**, *127*, 11851.
(44) Lebedev, A. Y.; Troxler, T.; Vinogradov, S. A. Design of metalloporphyrin-based dendritic nanoprobes for two-photon microscopy of oxygen. *J. Porphyrins Phthalocyanines* **2008**, *12*, 1261.
(45) Roussakis, E.; Spencer, J. A.; Lin, C.; Vinogradov, S. A. Two-photon antenna-core oxygen probe with enhanced performance. *Anal. Chem.* **2014**, *86*, 5937−5945.
(46) Dichtel, W. R.; Serin, J. M.; Edder, C.; Frechet, J. M. J.; Matuszewski, M.; Tan, L. S.; Ohulchanskyy, T. Y.; Prasad, P. N. Singlet oxygen generation via two-photon excited FRET. *J. Am. Chem. Soc.* **2004**, *126*, 5380.
(47) Esipova, T. V.; Rivera-Jacquez, H. J.; Weber, B.; Masunov, A. E.; Vinogradov, S. A. Two-photon absorbing phosphorescent metalloporphyrins: effects of π-extension and peripheral substitution. *J. Am. Chem. Soc.* **2016**, *138*, 15648.
(48) Finikova, O. S.; Cheprakov, A. V.; Vinogradov, S. A. Synthesis and luminescence of soluble *meso*-unsubstituted tetrabenzo- and tetranaphtho[2,3]porphyrins. *J. Org. Chem.* **2005**, *70*, 9562.
(49) Lebedev, A. Y.; Filatov, M. A.; Cheprakov, A. V.; Vinogradov, S. A. Effects of structural deformations on optical properties of tetrabenzoporphyrins: Free-bases and Pd complexes. *J. Phys. Chem. A* **2008**, *112*, 7723.
(50) Frisch, M. J.; Trucks, G. W.; Schlegel, H. B.; Scuseria, G. E.; Robb, M. A.; Cheeseman, J. R.; Scalmani, G.; Barone, V.; Mennucci, B.; Petersson, G. A.et al. *Gaussian 09*, Revision D.01; Gaussian, Inc.: Wallingford CT, 2009.
(51) Mikhailov, I. A.; Bondar, M. V.; Belfield, K. D.; Masunov, A. E. Electronic properties of a new two-photon absorbing fluorene derivative: The role of Hartree-Fock exchange in the density functional theory design of improved nonlinear chromophores. *J. Phys. Chem. C* **2009**, *113*, 20719.
(52) Andrae, D.; Haussermann, U.; Dolg, M.; Stoll, H.; Preuss, H. Energy-adjusted *ab initio* pseudopotentials for the 2nd and 3rd row transition elements. *Theor. Chim. Acta* **1990**, *77*, 123.
(53) Dunning, T. H.; Hay, P. J. Gaussian Basis Sets for Molecular Calculations. *Methods of Electronic Structure Theory* **1977**, *3*, 1.
(54) Nayyar, I. H.; Masunov, A. E.; Tretiak, S. Comparison of TD-DFT methods for the calculation of two-photon absorption spectra of oligophenylvinylenes. *J. Phys. Chem. C* **2013**, *117*, 18170.
(55) Masunov, A. E.; Mikhailov, I. A. Theory and computations of two-photon absorbing photochromic chromophores. *Eur. J. Chem.* **2010**, *1*, 142.
(56) Marenich, A. V.; Cramer, C. J.; Truhlar, D. G. Universal solvation model based on solute electron density and on a continuum model of the solvent defined by the bulk dielectric constant and atomic surface tensions. *J. Phys. Chem. B* **2009**, *113*, 6378.
(57) Zems, Y.; Moiseev, A. G.; Perepichka, D. F. Convenient synthesis of a highly soluble and stable phosphorescent Platinum porphyrin dye. *Org. Lett.* **2013**, *15*, 5330.
(58) Gentemann, S.; Medforth, C. J.; Forsyth, T. P.; Nurco, D. J.; Smith, K. M.; Fajer, J.; Holten, D. Photophysical properties of conformationally distorted metal-free porphyrins. Investigation into the deactivation mechanisms of the lowest excited singlet state. *J. Am. Chem. Soc.* **1994**, *116*, 7363.
(59) Gentemann, S.; Nelson, N. Y.; Jaquinod, L.; Nurco, D. J.; Leung, S. H.; Medforth, C. J.; Smith, K. M.; Fajer, J.; Holten, D. Variations and temperature dependence of the excited state properties of conformationally and electronically perturbed zinc and free base porphyrins. *J. Phys. Chem. B* **1997**, *101*, 1247.
(60) Sazanovich, I. V.; Galievsky, V. A.; van Hoek, A.; Schaafsma, T. J.; Malinovskii, V. L.; Holten, D.; Chirvony, V. S. Photophysical and structural properties of saddle-shaped free base porphyrins: Evidence for an "orthogonal" dipole moment. *J. Phys. Chem. B* **2001**, *105*, 7818.
(61) Chirvony, V. S.; van Hoek, A.; Galievsky, V. A.; Sazanovich, I. V.; Schaafsma, T. J.; Holten, D. Comparative study of the photophysical properties of nonplanar tetraphenylporphyrin and octaethylporphyrin diacids. *J. Phys. Chem. B* **2000**, *104*, 9909.
(62) Sommer, J. R.; Shelton, A. H.; Parthasarathy, A.; Ghiviriga, I.; Reynolds, J. R.; Schanze, K. S. Photophysical properties of near-infrared phosphorescent π-extended platinum porphyrins. *Chem. Mater.* **2011**, *23*, 5296.
(63) Haddad, R. E.; Gazeau, S.; Pecaut, J.; Marchon, J. C.; Medforth, C. J.; Shelnutt, J. A. Origin of the red shifts in the optical absorption bands of nonplanar tetraalkylporphyrins. *J. Am. Chem. Soc.* **2003**, *125*, 1253.
(64) Finikova, O.; Cheprakov, A.; Beletskaya, I.; Vinogradov, S. An expedient synthesis of substituted tetraaryltetrabenzoporphyrins. *Chem. Commun.* **2001**, 261.
(65) Finikova, O. S.; Cheprakov, A. V.; Beletskaya, I. P.; Carroll, P. J.; Vinogradov, S. A. Novel versatile synthesis of substituted tetrabenzoporphyrins. *J. Org. Chem.* **2004**, *69*, 522.
(66) Finikova, O. S.; Aleshchenkov, S. E.; Brinas, R. P.; Cheprakov, A. V.; Carroll, P. J.; Vinogradov, S. A. Synthesis of symmetrical tetraaryltetranaphtho[2,3]porphyrins. *J. Org. Chem.* **2005**, *70*, 4617.
(67) Cheprakov, A. V. The synthesis of π-extended porphyrins. In *Handbook of porphyrin science*; Kadish, K. M., Smith, K. M., Guilard, R., Eds.; World Scientific Publishing Co.: Singapore, 2011; Vol. *13*, p 1.
(68) Vicente, M. G. H.; Tome, A. C.; Walter, A.; Cavaleiro, J. A. S. Synthesis and cycloaddition reactions of pyrrole-fused 3-sulfolenes: A new versatile route to tetrabenzoporphyrins. *Tetrahedron Lett.* **1997**, *38*, 3639.
(69) Hopkins, P. B.; Fuchs, P. L. Chlorosulfenylation-dehydrochlorination reactions - a new and improved methodology for synthesis of unsaturated aryl sulfides and aryl sulfones. *J. Org. Chem.* **1978**, *43*, 1208.
(70) Sessler, J. L.; Mozaffari, A.; Johnson, M. R. *Organic Synthesis* **1998**, *70*, 68.
(71) Jentzen, W.; Song, X.-Z.; Shelnutt, J. A. Structural characterization of syntheitc and protein-bound porphyrins in terms of the lowest-frequency normal coordinates of the macrocycle. *J. Phys. Chem. B* **1997**, *101*, 1684.
(72) Shelnutt, J. A.; Song, X. Z.; Ma, J. G.; Jia, S. L.; Jentzen, W.; Medforth, C. J. Nonplanar porphyrins and their significance in proteins. *Chem. Soc. Rev.* **1998**, *27*, 31.
(73) Senge, M. O.; Medforth, C. J.; Forsyth, T. P.; Lee, D. A.; Olmstead, M. M.; Jentzen, W.; Pandey, R. K.; Shelnutt, J. A.; Smith, K. M. Comparative analysis of the conformations of symmetrically and asymmetrically deca- and undecasubstituted porphyrins bearing meso-alkyl or -aryl groups. *Inorg. Chem.* **1997**, *36*, 1149.
(74) Medforth, C. J.; Senge, M. O.; Smith, K. M.; Sparks, L. D.; Shelnutt, J. A. Nonplanar distortion modes for highly substituted porphyrins. *J. Am. Chem. Soc.* **1992**, *114*, 9859.
(75) Cheng, R. J.; Chen, Y. R.; Wang, S. L.; Cheng, C. Y. Crystal and molecular-structure of a 5-coordinate zinc complex of meso-tetraphenyltetrabenzoporphyrin. *Polyhedron* **1993**, *12*, 1353.

DOI: 10.1021/acs.jpca.7b04333
J. Phys. Chem. A 2017, 121, 6243−6255

(76) Finikova, O. S.; Cheprakov, A. V.; Carroll, P. J.; Dalosto, S.; Vinogradov, S. A. Influence of nonplanarity and extended conjugation on porphyrin basicity. *Inorg. Chem.* **2002**, *41*, 6944.
(77) Finikova, O. S.; Galkin, A. S.; Rozhkov, V. V.; Cordero, M. C.; Hagerhall, C.; Vinogradov, S. A. Porphyrin and tetrabenzoporphyrin dendrimers: Tunable membrane- impermeable fluorescent pH nanosensors. *J. Am. Chem. Soc.* **2003**, *125*, 4882.
(78) Kadish, K. M.; Finikova, O. S.; Espinosa, E.; Gros, C. P.; De Stefano, G.; Cheprakov, A. V.; Beletskaya, I. P.; Guilard, R. First highly distorted π-extended Fe(II) porphyrin - a unique model to elucidate factors affecting the electrochemical potentials. *J. Porphyrins Phthalocyanines* **2004**, *08*, 1062.
(79) Borek, C.; Hanson, K.; Djurovich, P. I.; Thompson, M. E.; Aznavour, K.; Bau, R.; Sun, Y. R.; Forrest, S. R.; Brooks, J.; Michalski, L.; et al. Highly efficient, near-infrared electrophosphorescence from a Pt-metalloporphyrin complex. *Angew. Chem., Int. Ed.* **2007**, *46*, 1109.
(80) Lebedev, A. Y.; Cheprakov, A. V.; Sakadzic, S.; Boas, D. A.; Wilson, D. F.; Vinogradov, S. A. Dendritic phosphorescent probes for oxygen imaging in biological systems. *ACS Appl. Mater. Interfaces* **2009**, *1*, 1292.
(81) Martinsen, J.; Pace, L. J.; Phillips, T. E.; Hoffman, B. M.; Ibers, J. A. Tetrabenzoporphyrinato)Nickel(II) Iodide - a doubly mixed-valence molecular conductor. *J. Am. Chem. Soc.* **1982**, *104*, 83.
(82) Liou, K.; Ogawa, M. Y.; Newcomb, T. P.; Quirion, G.; Lee, M. H.; Poirier, M.; Halperin, W. P.; Hoffman, B. M.; Ibers, J. A. Preparation, characterization and low-temperature transition of Cu(TBP)I, a new porphyrinic conductor with local moments coupled to itinerant charge-carriers. *Inorg. Chem.* **1989**, *28*, 3889.
(83) Liou, K. Y.; Newcomb, T. P.; Heagy, M. D.; Thompson, J. A.; Heuer, W. B.; Musselman, R. L.; Jacobsen, C. S.; Hoffman, B. M.; Ibers, J. A. Preparation and characterization of-(tetrabenzoporphyrinato)Cobalt(II) iodide, a ring-oxidized molecular conductor. *Inorg. Chem.* **1992**, *31*, 4517.
(84) Finikova, O. S.; Chen, P.; Ou, Z.; Kadish, K. M.; Vinogradov, S. A. Dynamic quenching of porphyrin triplet states by two-photon absorbing dyes: Towards two-photon-enhanced oxygen nanosensors. *J. Photochem. Photobiol., A* **2008**, *198*, 75.
(85) Rosa, A.; Ricciardi, G.; Baerends, E. J. Synergism of porphyrin-core saddling and twisting of *meso*-aryl substituents. *J. Phys. Chem. A* **2006**, *110*, 5180.
(86) Eastwood, D.; Gouterman, M. Porphyrins. XVIII. Luminescence of(Co),(Ni), Pd, Pt Complexes. *J. Mol. Spectrosc.* **1970**, *35*, 359.
(87) Callis, J. B.; Knowles, J. M.; Gouterman, M. Porphyrins. XXVI. Triplet excimer quenching of free base Zinc, Palladium, and Platinum Complexes. *J. Phys. Chem.* **1973**, *77*, 154.
(88) Vanderkooi, J. M.; Maniara, G.; Green, T. J.; Wilson, D. F. An optical method for measurement of dioxygen concentration based on quenching of phosphorescence. *J. Biol. Chem.* **1987**, *262*, 5476.
(89) Wilson, D. F.; Rumsey, W. L.; Green, T. J.; Vanderkooi, J. M. The oxygen dependence of mitochondrial oxidative phosphorylation measured by a new optical method for measuring oxygen. *J. Biol. Chem.* **1988**, *263*, 2712.
(90) Graham, K. R.; Yang, Y. X.; Sommer, J. R.; Shelton, A. H.; Schanze, K. S.; Xue, J. G.; Reynolds, J. R. Extended conjugation platinum(II) porphyrins for use in near-infrared emitting organic light emitting diodes. *Chem. Mater.* **2011**, *23*, 5305.
(91) Roussakis, E.; Li, Z. X.; Nowell, N. H.; Nichols, A. J.; Evans, C. L. Bright, "clickable" porphyrins for the visualization of oxygenation under ambient light. *Angew. Chem., Int. Ed.* **2015**, *54*, 14728.
(92) Strickler, S. J.; Berg, R. A. Relation between absorption intensity and fluorescence lifetime of molecules. *J. Chem. Phys.* **1962**, *37*, 814.
(93) De Boni, L.; Toro, C.; Masunov, A. E.; Hernandez, F. E. Untangling the excited states of DR1 in solution: An experimental and theoretical study. *J. Phys. Chem. A* **2008**, *112*, 3886.
(94) Masunov, A. E. Theoretical spectroscopy of carbocyanine dyes made accurate by frozen density correction to excitation energies obtained by TD-DFT. *Int. J. Quantum Chem.* **2010**, *110*, 3095.
(95) Iordanov, T. D.; Davis, J. L.; Masunov, A. E.; Levenson, A.; Przhonska, O. V.; Kachkovski, A. D. Symmetry breaking in cationic polymethine dyes, Part 1: Ground state potential energy surfaces and solvent effects on electronic spectra of streptocyanines. *Int. J. Quantum Chem.* **2009**, *109*, 3592.
(96) Le Guennic, B.; Jacquemin, D. Taking up the cyanine challenge with quantum tools. *Acc. Chem. Res.* **2015**, *48*, 530.

DOI: 10.1021/acs.jpca.7b04333
J. Phys. Chem. A 2017, 121, 6243−6255